On the altitude dependence of transversely heated O+ distributions in the cusp/cleft

M. Bouhram, B. Klecker, W. Miyake, H. Rème, J.-A. Sauvaud, M. Malingre, L. Kistler, A. Blagau

Annales Geophysicae (2004) 22: 1787–1798
SRef-ID: 1432-0576/ag/2004-22-1787

Annales Geophysicae

On the altitude dependence of transversely heated O^+ distributions in the cusp/cleft

M. Bouhram[1], B. Klecker[1], W. Miyake[2], H. Rème[3], J.-A. Sauvaud[3], M. Malingre[4], L. Kistler[5], and A. Blăgău[1,6]

[1]Max-Planck-Institut für extraterrestrische Physik, Gießenbachstraße, D-85741 Garching, Germany
[2]Communications Research Laboratory, 4-2-1 Koganei, Tokyo 184-8795, Japan
[3]CESR-CNRS, BP-4346, 31028 Toulouse Cedex 04, France
[4]CETP-CNRS, 4 Avenue de Neptune, 94100 Saint-Maur Cedex, France
[5]Space Science Center, University of New Hampshire, Durham, USA
[6]Space Science Institute, R-76911 Bucharest, Romania

Received: 11 September 2003 – Revised: 19 January 2004 – Accepted: 23 January 2004 – Published: 8 April 2004

Abstract. The present paper focuses on the altitude dependence of oxygen ion conics in the dayside cusp/cleft region. Here, combining oxygen data from the Akebono, Interball-2 and Cluster satellites allows, for the first time, one to follow the global development of energetic (up to ∼10 keV) ion outflow over a continuous and broad altitude range up to about 5.5 Earth radii (R_E). According to earlier statistical studies, the results are consistent with a height-integrated energization of ions at altitudes up to 3.5 R_E. Higher up, the results inferred from Cluster observations put forward evidence of a saturation of both a transverse energization rate and ion gyroradii. We suggest that such results may be interpreted as finite perpendicular wavelength effects (a few tens of km) in the wave-particle interactions. To substantiate the suggestion, we carry out two-dimensional, Monte Carlo simulations of ion conic production that incorporate such effects and limited residence times due to the finite latitudinal extent of the heating region.

Key words. Magnetospheric physics (auroral phenomena) – Space plasma physics (charged particle motion and acceleration; wave-particle interactions)

1 Introduction

Since the discovery of non-thermal O^+ ions at magnetospheric altitudes by Shelley et al. (1972), the study of mechanisms allowing these ions of ionospheric origin to enter the magnetosphere and their role in the magnetosphere dynamics has been an area of active research over the past three decades. Some recent reviews can be found in André and Yau (1997), and Moore et al. (1999). The largest fluxes of non-thermal (from 10 eV up to 10 keV) O^+ ions originate from the dayside cusp and cleft regions, as confirmed by earlier observations with DE-1 (Lockwood et al., 1985a, 1985b) and Viking (Thelin et al., 1990; Øieroset et al., 2000) satellites.

Inside the cusp/cleft, many satellite observations have revealed that ions, heated transversely to the geomagnetic field, escape from the Earth's gravity under the action of the mirror force and form so-called conics in velocity space (André and Yau, 1997). Two types of ion conics have been reported in the past literature. A first type, called standard or restricted ion conics, first reported by Sharp et al. (1977), has a peak flux in a direction oblique to the magnetic field (40–70°). The simplest explanation for their generation is a local, perpendicular energy transfer to cold ions. Such distributions have been mainly observed by sounding rockets, low and mid-altitude satellites (Sharp et al., 1977; Yau et al., 1983; Kintner et al., 1996; André et al., 1988; Whalen et al., 1991). A second type, called elevated or bi-modal conics, has been first identified by Klumpar et al. (1984). This type of conics has a peak flux located in an extended pitch angle domain at high energy, and with a significant up-going component at lower energy. Klumpar et al. (1984) attributed them to the presence of both upward acceleration and transverse energization of ions along the same geomagnetic field line. Another explanation was also proposed by Temerin (1986) and Chang et al. (1986), arguing that such distributions are the direct result of a height-integrated, transverse heating of ions as they move upward, the achieved perpendicular energy being progressively converted into parallel energy via the mirror force. Statistical studies of the evolution of ion conics versus altitude, from 8000 up to 24 000 km using DE-1 (Peterson et al., 1992) and below 10 000 km using Akebono

Correspondence to: M. Bouhram
(bouhram@mpe.mpg.de)

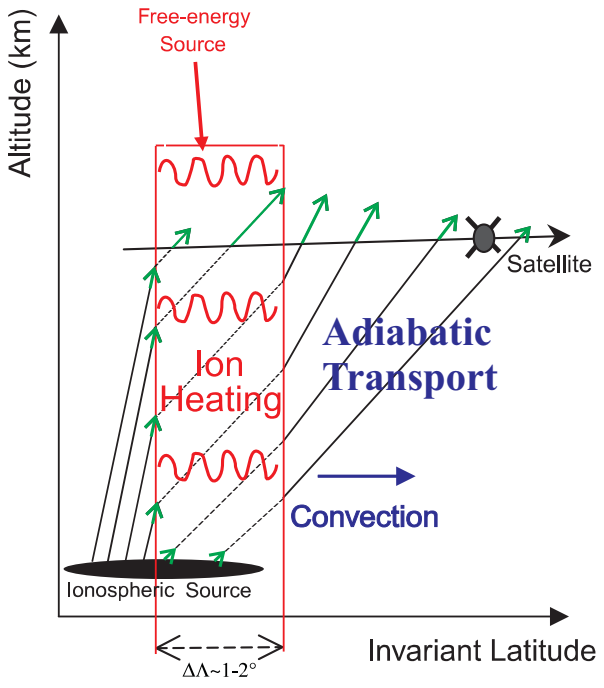

Fig. 1. Two-dimensional (invariant latitude-altitude) sketch that illustrates the transport patterns of ion outflows from an ionospheric source of finite latitudinal extent $\Delta\Lambda$ throughout the cusp/cleft and dayside polar cap, in conjunction with a high-altitude satellite pass. The green vectors correspond to the ion velocities and their lengths are proportional to their intensities.

data (Miyake et al., 1993, 1996) point out that, according to a height-integrated heating scenario, the characteristic energies of ion conics increase versus altitude, while their apex angle (the conic angle with respect to the upward direction) decreases much more slowly than expected from adiabatic folding. Heating mechanisms responsible for ion conic formation in the dayside cusp/cleft occur in a region extended in longitude, but well defined with a finite extent in latitude $\Delta\Lambda\sim$1–2°, often called the heating wall (Knudsen et al., 1994; Dubouloz et al., 1998). Hence, when observed at high-altitude and under the effect of the $\boldsymbol{E}\times\boldsymbol{B}$ convection drift, outflowing ions resulting from transverse heating spread out poleward of the cusp/cleft to form the so-called ion fountain (Lockwood et al., 1985b, Dubouloz et al., 1998). Figure 1 schematically summarizes the major physical processes responsible of the ion fountain formation. Poleward of the heating region, because of its finite latitudinal extent $\Delta\Lambda$, transverse energization is then followed by adiabatic magnetic pitch-angle folding of upward moving conics, along with a convective motion to form cold, upflowing ion beams of lower energy. The latter stage contributes to a velocity filter effect (Horwitz, 1986), as usually evidenced by the observation of a latitude-energy dispersion with any high-altitude satellite crossing the dayside cusp/cleft and polar cap (Lockwood et al., 1985b, Knudsen et al., 1994, Dubouloz et al., 1998). Basically, inside the heating region, the higher the achieved energy by a single ion, the lower its time needed to reach a high-latitude satellite. Conversely, ions weakly heated exit the heating region at lower altitude under the effect of the convection with the ion time of flight to reach the satellite being invertly proportional to its upward velocity, ions with lower energies are convected further away from the source region. This leads to the observation of continuous velocity-dispersed outflows along a satellite track, as shown in Fig. 1. Also, note that ion beams can be caused by both pitch-angle folding of moving conics and parallel electric fields (see André and Yau, 1997). However, the latter mechanism is associated with the auroral zone and unlikely occurs in the polar cap.

Because all major ion species achieve non-thermal energies when observed in the cusp/cleft, the most likely candidate for transverse energization is related to electric fields oscillating within some frequency range (see André and Yau, 1997 for a review). In the cusp/cleft and at the poleward edge of the auroral oval, recent statistical studies using FAST (Lund et al., 2000) and Freja (Hamrin et al., 2002) satellite data reported a strong link between ion conic events and enhancements of the broad-band extremely low frequency (BBELF) turbulence. Its spectral shape may be modeled by a power law profile versus frequency (Kintner, 1976), as parametrized by a spectral index α. Many wave modes may be contained in the BBELF turbulence and their relative contribution to the observed spectra is still under investigation (see Paschmann et al. (2002) for a review). However, in terms of transverse ion energization, several authors (Chang et al., 1986; Retterer et al., 1987; Crew et al., 1990, Norqvist et al., 1996; to name just a few) carried out one-dimensional (1D), Monte Carlo, kinetic simulations to point out that the observed conics can be explained by considering ion cyclotron resonance (ICR) heating over an extended altitude range with the electromagnetic left-hand circular polarized component (LHCP) of BBELF turbulence. It was confirmed that only a small fraction of the wave power at the ion gyrofrequency in the BBELF turbulence is needed to cause the observed ion energies. André et al. (1990) were the first to include the effect of the $\boldsymbol{E}\times\boldsymbol{B}$ convection drift. In their analysis, detailed wave and particle observations available for one event were used to carry out a 2-D, Monte Carlo simulation with a model according to Fig. 1. More recently, a 2-D, steady-state, trajectory-based code, similar to the one used by André et al. (1990), has been developed to investigate quantitatively the transport patterns of ion outflows from the dayside cusp/cleft associated with transverse heating by means of wave/particle interactions (Bouhram et al., 2003a). Introducing a convection drift leads to limited residence times of ions when being energized. In a companion paper (Bouhram et al., 2003b), by using high-altitude (1.5–3.0 R_E) ion observations on the Interball-2 satellite as constraints, the results of the numerical simulation studies were used to seek the altitude dependence of the ion heating rate below the satellite altitude for a significant number of passes in the cusp/cleft. It was pointed out that satellite observations

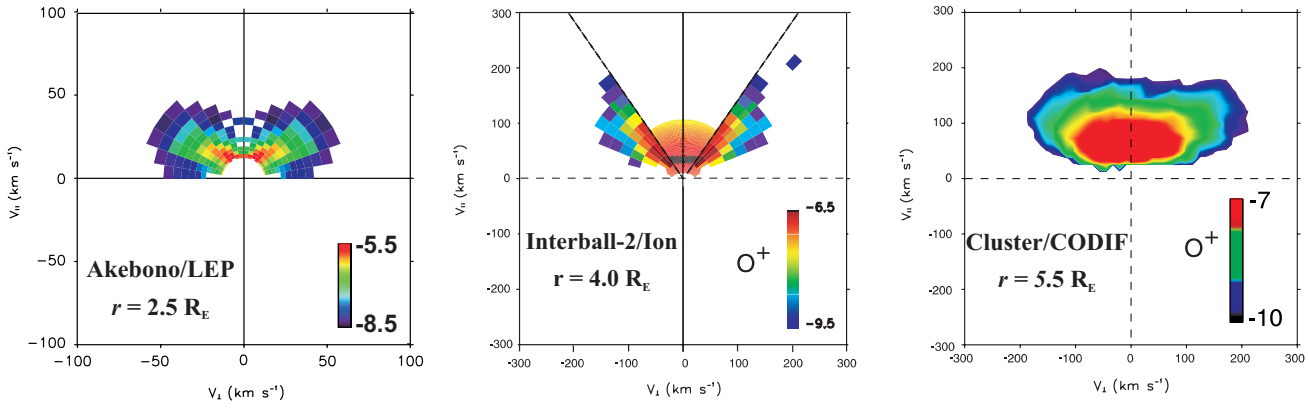

Fig. 2. From the left to the right, 3 examples of ion velocity distributions in $cm^{-3}\,km^{-3}\,s^3$ measured by Akebono/LEP at r=2.5 R_E, Interball-2/Ion at r=4.0 R_E, and Cluster/CODIF at r=5.5 R_E.

are consistent with a height-integrated ICR heating of ions, the ion heating rate following a power law versus geocentric distance as $r^{3.3\pm1.8}$. This study confirmed that only a small fraction (less than a few %) of the wave power typically observed in the BBELF spectrum is needed to reproduce high-altitude ion observations. On the other hand, it was found that the effect of parallel electric field is of minor importance, except in the pre-noon cleft region.

Understanding the global development in altitude of non-thermal, dayside, outflow of ionospheric origin is also needed to determine the ability of this latter component to supply in plasma the outer magnetospheric regions such as the magnetotail. Indeed, cold O^+ beams have been observed in the distant lobe/mantle region over a broad altitude range up to 210 R_E by the Geotail satellite (Hirahara et al., 1996; Seki et al., 1998, 2002). However, when comparing ion energies with those observed by low-altitude satellites in the cusp/cleft, it turns out that there is a need for extra energization of about 2.7 keV in between, for these ions to reach such large distances. As mentioned in Seki et al. (2002), O^+ observations in the high-altitude cusp region are needed to clarify this issue.

The present paper is an extension of the study by Bouhram et al. (2003a, b), gathering ion data in the cusp/cleft from Akebono, Interball-2 and Cluster satellites. The aim of this statistical study is to follow the altitude development of oxygen ion conics over a broad and complete altitude range, from the topside ionosphere up to about 5.5 R_E. Hence, we discuss the evolution of ion conics as a function of altitude at the poleward edge of the cusp/cleft and the possibility of finding out the altitude peak of the height-integrated heating of ions. Two-dimensional Monte Carlo simulations are used to explain qualitatively the statistical results.

2 Instrumentation and data analysis

In the present study, we utilized data from several satellites: Akebono, Interball-2, and three of Cluster spacecraft. In Sect. 2.1, we describe the instruments we used aboard those spacecraft. In Sect. 2.2, we present examples of ion distributions measured by such instruments. Finally, Sect. 2.3 describes how to select ion data at high-altitude for our purpose.

2.1 Instrumentation

The Akebono satellite was launched in 1989 into a polar orbit with an initial apogee of 10.482 km (1.6 R_E) and a perigee of 272 km. The low-energy particle (LEP) instrument (Mukai et al., 1990) aboard Akebono was designed to observe energy-pitch-angle distributions of auroral ions and electrons. It carries two sets of electrostatic (E/Q) analyzers separated at the symmetric position with respect to the satellite spin axis. The E/Q analyzers have 10 detectors, which were combined over a satellite spin period (7.5 s) to measure three-dimensional (3-D) distributions of ions and electrons, at energies ranging from 13 eV up to 20 keV for ions. In the present study, we only use ion data obtained by Akebono/LEP between April 1989 and March 1990, at solar maximum, and previously published by Miyake et al. (1993).

The Interball-2 satellite was launched in August 1996, into a 19.200×750 km orbit with 62.5° inclination. The ion instrument aboard Interball-2 has two detectors, i.e. two mass spectrometers, which use Wien filters to measure energy spectra of H^+, O^+ ions at higher energies (30 eV–15 keV) over two view directions rotating in the spin plane along with the satellite (Sauvaud et al, 1998). From Interball-2/Ion, 2-D ion distribution functions and moments are then recorded every spin period (120 s). Note also that Interball-2/Ion has two cylindrical spectrometers to measure electron distributions (see Sauvaud et al., 1998, for details). However, we only use in our study ion measurements by Interball-2/Ion in the cusp/cleft between January 1997 and April 1998, for solar minimum conditions, covering altitudes between 9000 and 19 200 km (e.g. 1.4 and 3.0 R_E, respectively), and previously discussed in Bouhram et al. (2003b).

Finally, the four identical Cluster satellites were launched in 2000 with an elliptical orbit (4.0×19.6 R_E) and an

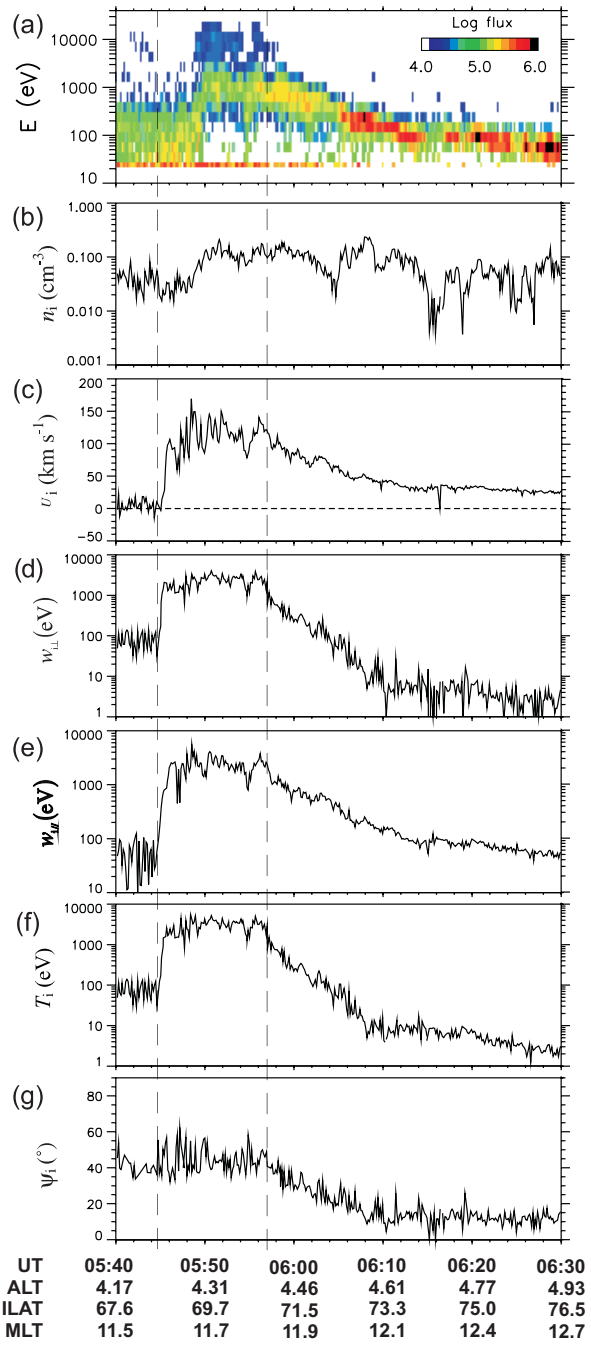

Fig. 3. Overview of a transverse O^+ ion heating event on 28 September 2001, between 05:40 and 06:30 UT: **(a)** time-energy spectrogram of O^+ ions, **(b)** O^+ ion density in cm^{-3}, **(c)** upward mean velocity in km s^{-1}, **(d)** perpendicular mean energy in eV, **(e)** parallel mean energy in eV, **(f)** temperature in eV, and **(g)** apex angle in °. The vertical dashed lines indicate the boundaries of the heating region.

inclination of 90°. Between July and November 2001, the Cluster fleet crossed the mid-altitude cusp/cleft region close to its perigee. Three-dimensional distributions of upflowing O^+ ions can be measured by the COmposition and DIstribution Function (CODIF) analyser, which is part of the Cluster ion spectrometry (CIS) package (Rème et al., 2001). CODIF operates aboard three of the four Cluster satellites, and measures 3-D distributions of the major ion species over the energy range 20–40 000 eV. It is a combination of a top-hat E/Q analyzer followed by a post acceleration of 15 kV and a time-of-flight measurement. The E/Q analyzer is divided into two halves, with geometric factor different by a factor of 100. Only one half operates at a time, giving a 180° instantaneous field-of-view divided into 8 sectors of 22.5° each. The E/Q analyzer sweeps through the full energy range 32 times per spin, so that the full distriution is obtained in one spin (4 s). In this study, O^+ data in the cusp/cleft from Cluster/CODIF, near solar maximum conditions, were used, covering altitudes from ∼3.0 up to 5.5 R_E. Hence, using such instruments together, we can thus obtain complete altitude coverage of the cusp/cleft up to about 5.5 R_E.

2.2 Examples of data

Figure 2 shows three examples of ion conics measured by the instruments utilized in the present study. The first ion distribution of Fig. 2 (left) is recorded by the Akebono/LEP instrument. It is made from the integration of 15-s observations and is sorted into 29×18 energy-pitch angle bins, assuming that all ions are O^+. The next O^+ion distribution of Fig. 2 (center) is recorded by the Interball-2/Ion instrument. It is made from the integration of 120-s observations and is sorted into 16×16 energy-pitch angle bins. Note when the satellite is in the auroral and polar regions, an angle appears between the geomagnetic field and the spin plane of the detectors. Therefore, the parallel and anti-parallel directions are not scanned. Usually, only pitch angles between 30° and 150° are scanned by the detectors, as evidenced in Fig. 2 (center). When studying ion conics, the filling-in procedure (Bouhram, 2002) has been applied to fit the missing portion in angle. The last O^+ion distribution of Fig. 2 (right) is recorded by CODIF aboard one Cluster satellite. It is made from the integration of 4-s observations using 16×8×32 energy-detector-spin angle bin measurements. Note that in our study, only moments inferred from ion distributions are used statistically, as discussed below.

2.3 Selecting data at high-altitude

As discussed in Sect. 1, Fig. 1, at high-altitude, such as those covered by Interball-2 and Cluster, because of the finite latitudinal extent of the heating region, the conjugate action of ion heating processes and transport mechanisms (adiabatic folding, convection) leads to the observation of ion conics and cold beams throughout the cusp/cleft and polar cap, respectively. Hence, to seek the altitude dependence of ion energization in the cusp/cleft, it is more convenient to consider only data along the downstream edge of the heating region. Figure 3 shows a typical example of O^+ ion outflow observations during a high-altitude cusp/cleft pass by one Cluster satellite under relatively steady solar wind conditions, with

negative B_z and B_y interplanetary magnetic field (IMF) components in geocentric solar magnetic (GSM) coordinates. Cluster crosses the equatorward edge of the heating region at 05:45 UT, as evidenced by a sudden increase in the O^+ ion mean energy components $w_{i//}$, $w_{i\perp}$ and temperature T_i. Poleward of this boundary, the increase in the upward mean velocity u_i and temperature T_i indicate that ion distributions are folded upward to form elevated conics of ~1 keV energy with a high-energy tail extending up to tens of keV (see Fig. 3a). This is consistent with a height-integrated transverse heating of ions as far as they convect poleward through the wall. According to numerical simulation studies (see Bouhram et al., 2003a, b), the crossing of the poleward heating boundary occurs at about 05:57 UT, right before all the first and second order moments (e.g. u_i, $w_{i//}$, $w_{i\perp}$ and T_i) drop precipitously. After 05:57 UT, the decrease in the apex angle (or conic angle) defined by Ψ_i=arctan$[(w_{i\perp}/w_{i//})^{1/2}]$ indicates that because of the lack of transverse energization, conics fold up into beams adiabatically. As discussed in Sect. 1 (see also Fig. 1), this latter stage, in combination with the poleward convection, contributes to a velocity filter effect as evidenced by the time-of-flight dispersion in the ion spectrogram or in the evolution of u_i and $w_{i//}$. Note that for northward IMF conditions, because the convection is sunward in the cusp, the previous picture is basically reversed in latitude and the downstream heating boundary then corresponds to the equatorward edge of the cusp/cleft. In short, for any high-altitude pass in the dayside, data at the downstream edge of the heating region can be selected by simply keeping the most energetic ion conics. This procedure has been applied to Interball-2 and Cluster data for this study.

3 Altitude survey: Akebono/Interball-2/Cluster intercomparison

For any transverse heating event, restricted to the dayside cusp/cleft region for MLTs between 9.0 and 15.0 h, we keep the most energetic ion conics (e.g. those observed at the poleward edge of the heating region), as previously discussed in Sect. 2.2. For making intercomparison, ion moments, such as those of Fig. 3, are derived from ion distributions. Unfortunately, for the Akebono/LEP database, used in Miyake et al. (1993), only the temperature and the apex angle of ion conics are available. Figure 4 shows the number of ion conics per altitude range and the scatterplots of ion moments as a function of geocentric distance r. In the present study, we have averaged CODIF ion distributions over 60 s, in order to make the number of data points of about the same order as for the Interball-2/Ion and Akebono/LEP databases. During these events, the three Cluster satellites SC1, SC3, and SC4, on which CODIF data are available, are highly separated. The time lag with respect to the leading satellite SC4 is about 5 min and 40 min for SC1 and SC3, respectively. When comparing this time lag with typical times-of-flight of non-thermal O^+ ions (a few minutes for energies above 100 eV) to reach Cluster, it turns out that data points from

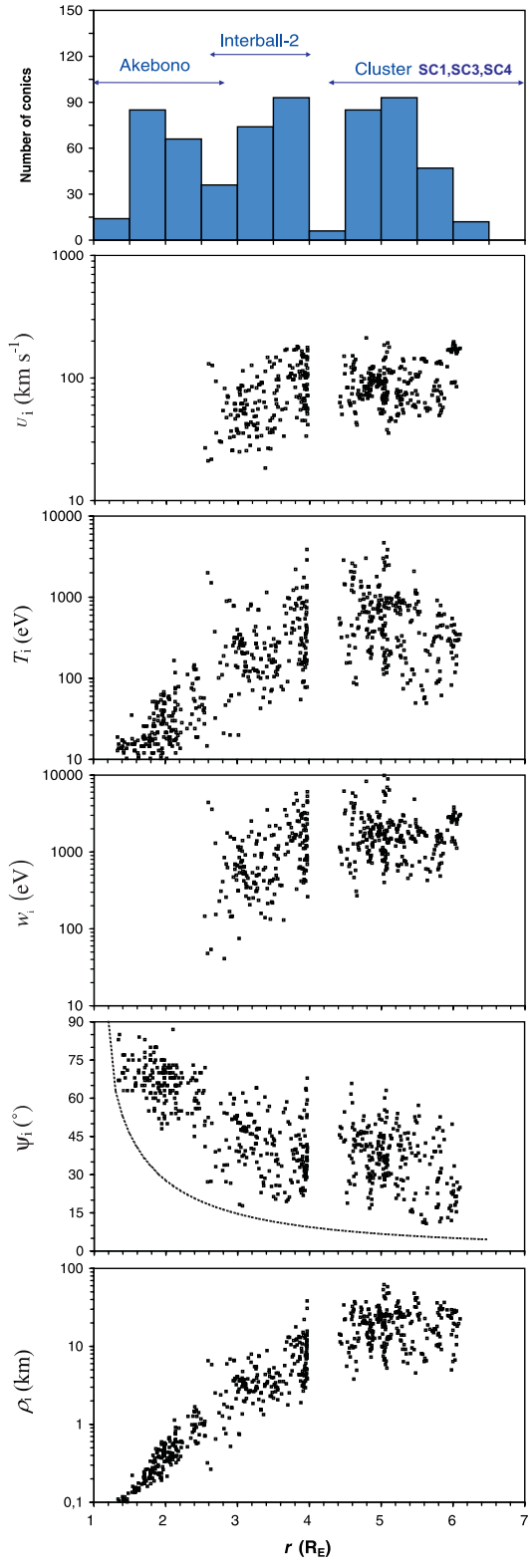

Fig. 4. From top to bottom, number of ion conical distributions per altitude range, and scatterplots of different oxygen ion quantities: upward mean velocity in km s^{-1}, temperature in eV, mean energy in eV, apex angle in °, and mean gyroradius in km.

SC3 should be statistically independent of data from SC1 and SC4, while data from SC1 and SC4 may be dependent. We should note that a narrow gap in the range r=4.0−4.4 R_E appears in Fig. 4 right above Interball-2 apogee, which is related to the Cluster orbit. Indeed, Cluster has an elliptical orbit (4.0×19.6 R_E) with a high inclination and its perigee close to the equatorial plane. Therefore, cusp/cleft crossings by Cluster occur slightly higher than at 4.0 R_E, from about 4.4 R_E.

For all scatterplots in Fig. 4, we can see a good continuity between data points obtained by Akebono/LEP (<2.6 R_E), Interball-2/Ion (2.5–4.0 R_E), and Cluster/CODIF (4.4–6.2 R_E). Here, we remind the reader that Akebono/LEP and Cluster/CODIF data are available for solar maximum conditions, whereas Interball-2/Ion data were taken at solar minimum. Therefore, the good continuity for first and second order O^+ moments in Fig. 4 implies that transverse energization mechanisms in the cusp/cleft are not solar cycle dependent. On the other hand, we found a discontinuity in the O^+ density (not shown), measurements by Interball-2/Ion at 4.0 R_E being on average less than one order of magnitude lower than those from Cluster/CODIF at 4.4 R_E. Because O^+ fluxes at solar minimum are known to be statistically a factor of 5 lower than those at solar maximum (Yau et al., 1988), this discontinuity is not surprising and can be simply understood in terms of solar cycle effects.

For geocentric distances r<4.5 R_E, as expected in the case of a height-integrated heating scenario, the bulk velocity u_i, the ion temperature T_i and the ion mean energy w_i increase gradually versus r, while the apex angle Ψ_i is found to decrease much more slowly than expected from adiabatic folding. In Fig. 4d, we plotted using a dotted line the evolution of Ψ_i when assuming transverse energization at low altitude followed by an adiabatic motion, which means that sin Ψ_i is proportional to $r^{-1.5}$. When fitting the data points by the same kind of power law dependence, we find that sin Ψ_i is proportional to $r^{-0.6}$ with a correlation coefficient R=0.7. This result is simply a consequence of the accumulation of perpendicular energy by ions along the field line, which slows down the folding of ion conics. We also plotted in Fig. 4e, the ion mean gyroradius ρ_i, which is proportional to $T_{i\perp}^{1/2}/B$ or also $r^3 T_{i\perp}^{1/2}$. For Akebono/LEP data points, we neglected $T_{i//}$ and assumed $T_{i\perp}$∼1.5 T_i. The steep increase in $\rho_i(r)$ is also consistent with a height-integrated heating scenario rather than the possibility that ion conics are created at arbitrary altitudes by means of explosive energization processes.

For geocentric distances r>4.5 R_E, in the range covered by Cluster, the ion temperature T_i starts to decrease versus r. A similar behavior was found for the perpendicular temperature (not shown) using Cluster/CODIF data only. Another counterintuitive result found in Fig. 4 is that the bulk velocity u_i, the ion mean energy w_i and the mean ion gyroradius ρ_i exhibit a flat evolution above 4.5 R_E, with typical values of about 50–150 km/s^{-1}, 0.5-5 keV, and 5–50 km, respectively. We should mention here that the observed finite gyroradius could not be explained by the finite latitudinal extent of the heating region. Indeed, the thickness of the heating wall is typically of about 1–2° (Dubouloz et al., 1998; Valek et al., 2002), which corresponds to a perpendicular distance of 1000–2000 km at 4.5 R_E, for example, more than one order of magnitude higher than the maximum values observed for ρ_i.

In short, such results suggest that the strength of ion transverse heating starts to saturate beyond r∼4.5 R_E. We will show in the next section that, if assuming ion cyclotron resonant (ICR) heating by means of left-hand circular polarized (LHCP) waves as the dominant energization mechanism, this may be interpreted as the result of finite wavelength effects in ion heating.

4 Comparison with an ion heating model

The statistical results of the altitude behavior of all quantities at the poleward edge of the cusp/cleft cannot be discussed quantitatively without some computer modeling. In the present section, we summarize different properties of the ICR heating theory and carry out a few kinetic Monte Carlo simulations to be compared with the scatterplots inferred from satellite data.

4.1 ICR heating theory

The transverse heating of ions can be treated in terms of the weak turbulence theory, where the ion heating results from the exchange of energy between the ions and the waves. As confirmed by many observations and numerical simulation studies (Chang et al., 1986; Retterer et al., 1987; André et al., 1990), the ions can interact with broad-band extremely low-frequency (BBELF) waves via the resonance at the ion gyrofrequency Ω_i. In the presence of such turbulent electric field spectra, the resonant effects on the ion distribution $f_i(\boldsymbol{r},\boldsymbol{V},t)$ in the phase space $(\boldsymbol{r},\boldsymbol{V})$ can be described by the kinetic equation (Ichimaru, 1973):

$$\left\{\frac{\partial}{\partial t}+\boldsymbol{V}\cdot\frac{\partial}{\partial \boldsymbol{r}}+\boldsymbol{F}\cdot\frac{\partial}{\partial \boldsymbol{V}}\right\} f_i(\boldsymbol{r},\boldsymbol{V},\boldsymbol{t}) =$$

$$\frac{\partial}{\partial \boldsymbol{V}}\cdot\boldsymbol{D}_i\cdot\frac{\partial}{\partial \boldsymbol{V}} f_i(\boldsymbol{r},\boldsymbol{V},\boldsymbol{t}), \quad (1)$$

where $\boldsymbol{F}$ denotes the macroscopic forces, and q_i and m_i are the ion charge and mass, respectively. The right-hand side of Eq. (1) expresses the heating of ions resulting from the wave-particle interactions, as described by a quasi-linear velocity diffusion tensor $\boldsymbol{D}_i$, which depends on the spectral density of the electric field turbulence as a function of frequency ω and wave vector $\boldsymbol{k}$. In our problem, the largest contribution to the integral over the spectral density to $\boldsymbol{D}_i$ comes from its perpendicular component $D_\perp$. Therefore, Eq. (1) may be simplified by keeping only this contribution. Applying the weak turbulence theory to this cyclotron interaction,

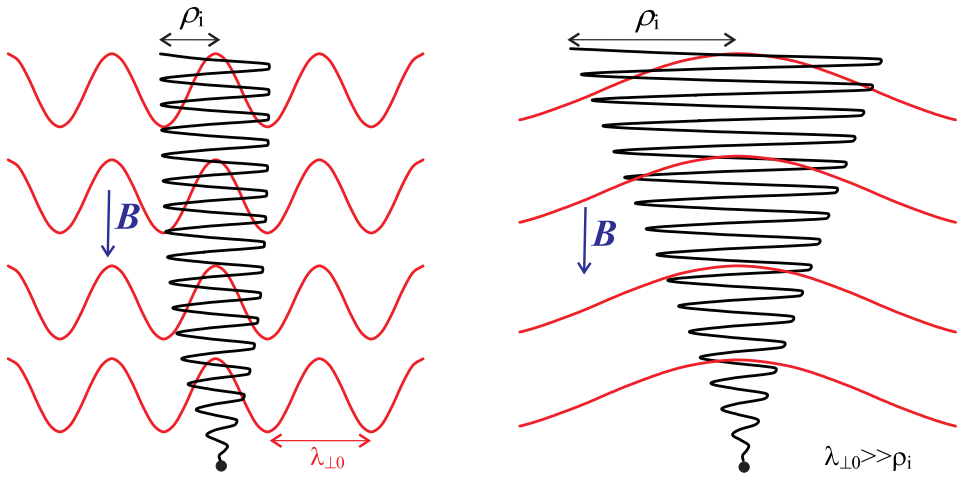

Fig. 5. Microscopic illustration of the gyrating motion of a single ion (black curve) across a wave field (red curves) transverse to the magnetic field (B) when (left) the ion gyroradius ρ_i is of the order of the perpendicular wavelength $\lambda_{\perp 0}$ of the structures, and (right) in the case of large perpendicular scale structures ($\rho_i << \lambda_{\perp 0}$).

Table 1. List and values of parameters of Monte Carlo simulations computed for the present study.

Run Id.	Residence time t_D	Heating rate at $r=r_0$	Spectral index α	Perpendicular wavelength $\lambda_{\perp 0}$
1	500 s	0.3 eV s^{-1}	1.1	$+\infty$
2	500 s	0.3 eV s^{-1}	1.1	100 km
3	500 s	0.3 eV s^{-1}	1.1	50 km
4	500 s	0.3 eV s^{-1}	1.1	10 km
5	500 s	1.0 eV s^{-1}	0.6	50 km
6	500 s	0.1 eV s^{-1}	1.7	50 km

we can infer from $D_\perp$ a perpendiular ion heating rate which can be expressed as (Brambilla, 1996) :

$$\dot{W}_{i\perp} = 2m_i D_\perp = \frac{\pi q_i^2}{2m_i} \int \frac{d\boldsymbol{k}}{(2\pi)^3} \sum_n \delta(\omega - n\Omega_i - k_{//} V_{//})$$

$$\times \left(1 - \frac{k_{//} V_{//}}{\omega}\right) \left[E_L J_{n-1}\left(\frac{k_\perp V_\perp}{\Omega_i}\right) + E_R J_{n+1}\left(\frac{k_\perp V_\perp}{\Omega_i}\right)\right]^2, \quad (2)$$

where $k_{//}$ and $k_\perp$ are the parallel and perpendicular components of the wave vector k. E_L and E_R denote the polarized left- and right-handed components of the oscillating electric field in the Fourier's space, respectively. It is important here to note that the expression for the previous quantities are weighted by modified Bessel functions $J_{n\pm1}$, which emphasizes the lower n values, in particular the fundamental n=1.

A difficulty in applying Eq. (1) is that it depends on the details of the ion distribution and the wave spectrum, especially in space plasmas, where detailed information on the k spectrum is unavailable. Under these circumstances, to take into account first-order finite wavelength corrections, we may keep the fundamental term and neglect terms at the harmonics of the gyrofrequency. If assuming a monochromatic wave at ω=Ω_i with a perpendicular wave number $k_{\perp 0}$, and the Doppler shift being usually small (e.g. $k_{//} V_{//} << \Omega_i$), we obtain the expression:

$$\dot{W}_{i\perp} = \frac{q_i^2 S_L}{2m_i} J_0^2(k_{\perp 0}\rho_i), \quad (3)$$

where S_L is the left-hand component of the electric field spectral density in V^2 m^{-2} Hz^{-1} at ω=Ω_i, and ρ_i=$V_\perp/\Omega_i$ denotes the ion gyroradius. In Eq. (3), the term J_0 tends to lower the heating rate, particularly after it matches its first zero for $k_{\perp 0}\rho_i \sim 2.4$. This means that ions cannot reach locally perpendicular velocities associated with a gyroradius ρ_i higher than the transverse spatial scale (perpendicular wavelength) of the waves $\lambda_{\perp 0}$=$2\pi/k_{\perp 0}$; Brambilla (1996). The left-hand side of Fig. 5 illustrates this effect on the gyrating motion of a single particle in a microscopic view. Conversely, the right-hand side of Fig. 5 describes the interaction of a single particle with waves of perpendicular wavelength greater than the ion gyroradius. According to Eq. (3), in the infinite wavelength limit, e.g. $k_{\perp 0}\rho_i << 1$, $J_0 \sim 1$, we obtain the expression derived by Chang et al. (1986) which does not depend on the ion velocity and therefore does not constrain the ion gyrating motion to the perpendicular scale size of the structures.

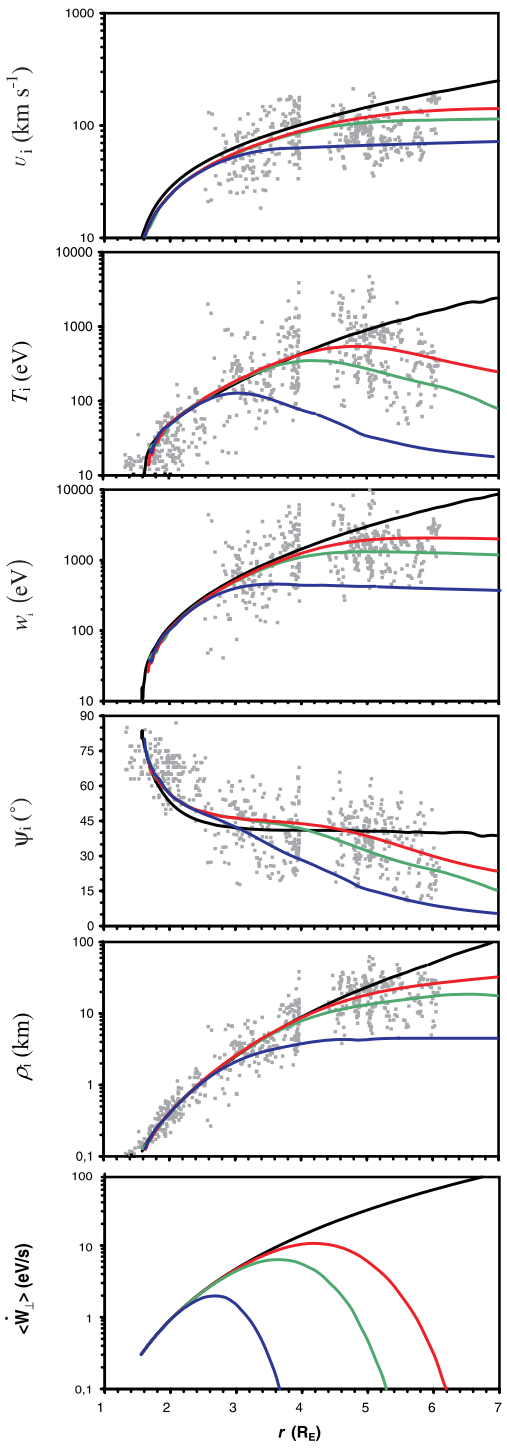

Fig. 6. Comparison along the poleward edge of the cusp/cleft between scatterplots of O^+ quantities and those obtained from numerical simulations. From top to bottom, upward mean velocity in km s^{-1}, temperature in eV, mean energy in eV, apex angle in °, mean gyroradius in km, and velocity-averaged heating rate in eV s^{-1}. Blue, green, red, and black curves correspond to different values of the perpendicular wavelength: 10 km, 50 km, 100 km, and infinity, respectively. All other simulation parameters are summarized in Table 1 (i.e. run 1 to run 4).

4.2 Monte Carlo simulations

To reproduce the statistical results on the altitude behaviour of oxygen ion conics, two-dimensional (2-D) Monte Carlo simulations have been carried out. This was accomplished using the 2-D, steady-state, trajectory-based code developed by Bouhram et al. (2003a). The code geometry is the same as in the sketch of Fig. 1. We model the transport patterns of non-thermal O^+ flows, associated with transverse heating by means of wave-particle interactions (by ion cyclotron resonance) and in combination with the poleward motion due to the magnetospheric convection. The effect of the convection drift is parametrized by a finite residence time t_D of ions when being energized. Since all computer particles are launched at the equatorward (or upstream) edge of the heating region, the parameter t_D also corresponds to the time needed to cross the heating region. According to earlier studies (Bouhram et al., 2003a), only the ion density and quantities weighted by the density, such as the particle flux or the energy density flux, are affected by residence time effects but not moments of 1st and 2nd order.

In this study, reproducing the altitude behaviour of ion distributions is a matter of choosing the ion energization altitude profile. According to earlier studies (Chang et al., 1986; André et al., 1990; Bouhram et al., 2003a, b) and to incorporate finite wavelength effects (see Sect. 4.1), we use for the ion heating rate at a geocentric distance r the expression as follow:

$$\dot{W}_{i\perp}(r,\rho_i) = \dot{W}_{i\perp}(r_0) \times \left(\frac{r}{r_o}\right)^{3a} J_0^2\left(2\pi\frac{\rho_i}{\lambda_{\perp o}}\right), \qquad (4)$$

where $\lambda_{\perp 0}=2\pi/k_{\perp 0}$ denotes the perpendicular wavelength of the wave turbulence, and α the spectral index associated with the LHCP component in the BBELF spectrum. In the model, the perpendicular energization of a computer particle is modeled as a series of random perpendicular velocity kicks according to Eq. (4). For a position r in the heating region, we can also infer a velocity averaged heating rate $<\dot{W}_{i\perp}>(\boldsymbol{r})$, as defined by:

$$<\dot{W}_{i\perp}>(\boldsymbol{r}) = (1/n_i(\boldsymbol{r}))\iiint \dot{W}_{i\perp}(\boldsymbol{r},\rho_i)\, f_i(\boldsymbol{r},\boldsymbol{V})\, d^3\boldsymbol{V}, \qquad (5)$$

where $f_i(r,V)$ and n_i are the steady-state distribution function and local density, respectively.

Table 1 summarizes the simulation parameters and their values for different runs. The lower and upper boundaries of our simulation system in r are about 1.3 R_E and 7.0 R_E, respectively. For each run, about 2×10^5 computer particles are launched along the equatorward heating boundary with a density profile proportional to r^{-3} to satisfy the flux conservation of ion densities.

Figure 6 shows a comparison between simulated profiles along the downstream heating boundary and the scatterplots of all ion quantities inferred from Akebono/LEP, Interball-2/Ion and Cluster/CODIF by considering different values of the perpendicular wavelength $\lambda_{\perp 0}$. Below 3–4 R_E, the ion

gyroradius is small enough so that finite wavelength effects are negligible in Eq. (4), and therefore all the models exhibit the same profile for any O^+ moment. For a fixed wavelength $\lambda_{\perp 0}$ the transition region where finite wavelength effects start to be nonnegligible corresponds basically to the altitude range where the velocity-averaged heating rate $<\dot{W}_{i\perp}>(\boldsymbol{r})$ does not increase anymore (last panel). Depending on $\lambda_{\perp 0}$, this transition region ranges between 3 and 4 R_E in geocentric distance. Above 4.0 R_E, we see that the altitude profile model with $\lambda_{\perp 0}$=50–100 km reproduces quite well the behavior of all scatterplots versus r. In particular, the O^+ temperature exhibits a flat peak at 4.1 R_E and the mean gyroradius does not exceed 30 km. Conversely, the other models for infinite or smaller (<50 km) wavelengths have severe problems in reproducing some of the features in the scatterplots (see, for example, the gyroradius and temperature profiles).

We also investigated the influence of the power law index α on the results for a fixed perpendicular wavelength. Figure 7 shows a comparison between simulated profiles along the downstream heating boundary and the scatterplots of all ion quantities inferred from Akebono/LEP, Interball-2/Ion and Cluster/CODIF for $\lambda_{\perp 0}$=50 km and by considering different heating rate profiles (see Table 1). The values for α were chosen according to earlier statistical studies to fit observations below 4 R_E, e.g. α=1.1±0.6 (Bouhram et al., 2003b). We can see that once again, the behavior of all scatterplots is reasonably well reproduced. In particular, the temperature is found to exhibit a peak ranging from 3.8 to 4.2 R_E, and a similar result is found for the peak of $<\dot{W}_{i\perp}>(\boldsymbol{r})$. This means that this position depends weakly on the heating rate profile at low altitude.

5 Discussion

The present statistical study, which combines oxygen ion data from Akebono, Interball-2 and three Cluster satellites, allows, for the first time, one to follow the global development of non-thermal O^+ outflow over a broad range of geocentric distances r up to 6.5 R_E, and therefore to infer empirical relationships as a function of altitude.

In this study, we have confirmed previous results, such as the fact that transverse ion heating in the cusp/cleft is height-integrated at radial distances below 4 R_E. In particular, intercomparison between Akebono data below 2.6 R_E and Interball-2 data between 2.5 R_E and 4 R_E exhibits a remarkable continuity as a function of altitude. Since these data were taken at different phases of the solar cycle, such results imply that transverse energization mechanisms are not solar cycle dependent. This means that the source of free energy comes from the magnetosphere or solar wind, while the ionosphere acts as a provider of O^+ ions to follow the continuity of the flow. For the first time, a statistical analysis above r=3 R_E put forward evidence that the cusp/cleft may act as a source of O^+ ions at energies of a few keV, for example, comparable to those of trapped particles, which can

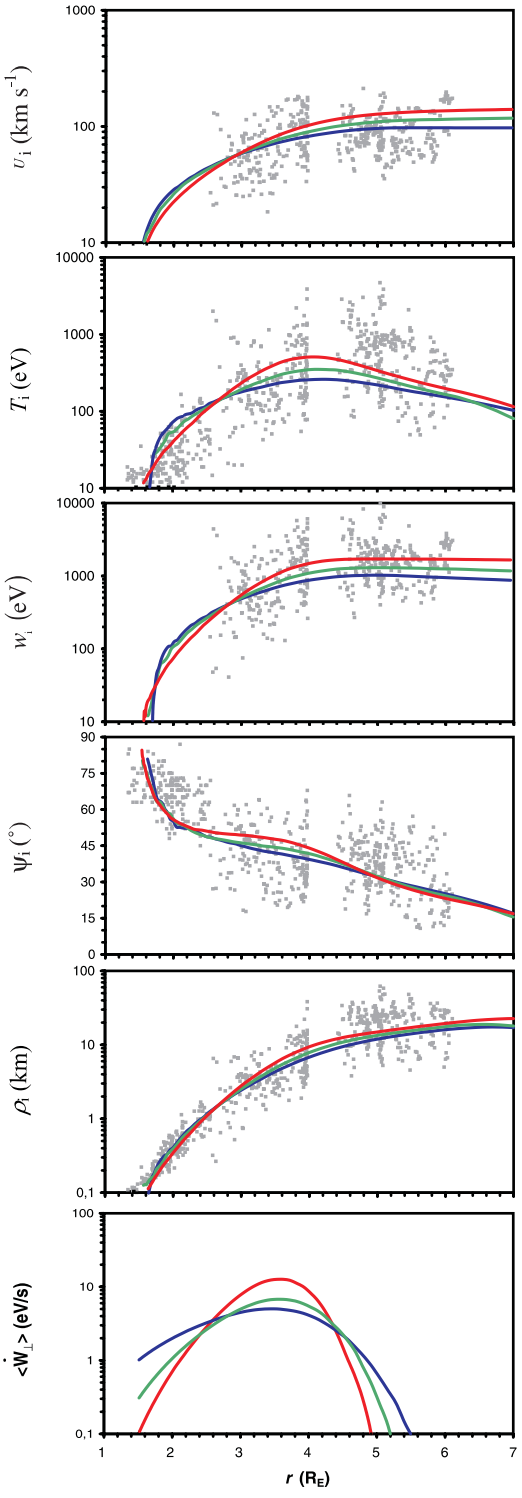

Fig. 7. Comparison along the poleward edge of the cusp/cleft between scatterplots of O^+ quantities and those obtained from numerical simulations for a perpendicular wavelength of 50 km and different heating profiles. The green, blue, and red curves are associated with runs 3,5, and 6, respectively (see Table 1). The O^+ quantities are the same as those of Fig. 6.

reach large distances in the magnetotail, as recently reported from observations by Geotail (Seki et al., 1998, 2002).

At radial distances $r>4.5\,R_E$, the survey using Cluster data indicated a decrease in O^+ temperature, while O^+ gyroradii do not exceed a few tens of kilometers, which means that a saturation of transverse heating processes occurs. The results of two-dimensional Monte Carlo kinetic simulations point out that limited O^+ gyroradii may be interpreted as the consequence of finite-wavelength effects of about a few tens of kilometers in the heating of ions. This has been accomplished by adopting an altitude heating rate profile accordingly. Since direct information on the (ω,k) spectrum is not available, another alternative explanation for the drop in the strength of ion heating above $r>4.5\,R_E$ may be a lack of wave power in the LHCP mode at gyrofrequencies below 0.6 Hz that leads to a similar altitude heating rate profile. Low-frequency electromagnetic waves exhibiting a broad-band or power law spectrum have been observed in the high-altitude cusp by Polar (Le et al., 2001) and Cluster (Opgenoorth et al., 2001, Cornilleau-Wehrlin et al., 2003) satellites. However, no statistical study on the altitude dependence in this range has been done yet. Therefore, we cannot completely rule out this latter possibility. For further investigation, detailed information on the (ω,k) spectrum and its altitude dependence need to be used as discussed below.

Although the energization of O^+ ions in the cusp/cleft is known to be associated with electric field fluctuations in a low-frequency domain (<10 Hz), the origin of the waves is still under investigation, for example, whether they are locally generated or propagate down from the magnetospheric boundary region. However, since transverse ion heating occurs in a broad altitude range and is found to be partly controlled by the B_y and southward B_z GSM components of the IMF, many authors suggested that the waves responsible of ion heating can be generated higher up in the dayside reconnection region (Peterson et al., 1993; Miyake et al., 2000, Bouhram et al., 2003b). A recent statistical study of electric field fluctuations below 4.0 Hz with Akebono data ($r<2.6\,R_E$) by Miyake et al. (2003) suggests that the turbulence may be more likely interpreted in terms of Alfvén waves centered in the cusp/cleft region and propagating down to lower altitudes, but should also be possibly attributed to more than one single mechanism (e.g. quasi-steady reconnection). On the other hand, recent observations with the Polar satellite (Le et al., 2001) showed that electromagnetic waves with a peak around the H^+ gyrofrequencies (0.2–4.0 Hz) are a permanent feature in the high-altitude cusp (6–9 R_E). Their statistical survey indicates that these waves are found in both equatorward and poleward edges of the cusp and in the cusp itself, with highly variable properties, but with a downward Poynting flux into the ionosphere, and are likely to be generated by precipitating magnetosheath plasma. Since these waves have frequencies equal to O^+ gyrofrequencies in a range $r\sim$2.5–6.5 R_E and a Poynting flux pointing downward, they may be able to induce transverse energization at lower-altitude. However, since the previous studies do not contain information on the (ω,k) spectrum, the true nature of the waves remains an open issue that needs to be clarified.

Recently, using magnetic field wave measurements aboard the four Cluster satellites in a short separation configuration ($\sim$100 km), Sahraoui et al. (2003) used the k-filtering technique developped by Pinçon and Lefeuvre (1992) to infer the (ω,k) spectrum of the magnetic turbulence in the magnetosheath for wavelengths higher than the separation distance and frequencies ranging from 0.3 to 3.0 Hz. To check our interpretation, such techniques may be applied, to a few cases in the high-altitude cusp region (8.0–10.0 R_E) to analyze the properties of this electromagnetic turbulence and possibly to study its propagation along the cusp field lines and its ability to interact with heavy ions of ionospheric origin.

Acknowledgements. The work at MPE (Max-Planck-Institut für Extraterrestrische Physik) in Garching is supported by DLR (Deutsches Zentrum für Luft und Raumfahrt) under contract 50 OC 0102. The Interball project was accomplished in the frame of contract N025-7535/94 with the Russian Space Agency (RSA). W. Miyake thanks all the members of Akebono project team, especially K. Tsuruda, H. Oya, and T. Mukai, for their extensive support.

Topical Editor T. Pulkkinen thanks a referee for his help in evaluating this paper.

References

André, M., Matson, L., Koskinen, H., and Erlandson, R.: Local transverse ion energization in and near the polar cusp, Geophy. Res. Lett., 15, 107–110, 1988.

André, M., Crew, G. B., Peterson, W. K., Persoon, A. M., Pollock, C. J., and Engebretson, M. J.: Ion heating by broadband low-frequency waves in the cusp/cleft, J. Geophy. Res., 95, 20 809–20 823, 1990.

André, M. and Yau, A. W.: Theories and observations of ion energization and outflow in the high latitude magnetosphere, Space Sci. Rev., 80, 27–48, 1997.

Bouhram, M.: Etude des échappements d'ions du côté jour des zones aurorales, PHD thesis, Univ. Pierre and Marie Curie, Paris, France, 2002.

Bouhram, M., Malingre, M., Jasperse, J. R., and Dubouloz, N.: Modeling transverse heating and outflow of ionospheric ions from the dayside cusp/cleft: 1 A parametric study, Ann. Geophys., 21, 1753–1771, 2003a.

Bouhram, M., Malingre, M., Jasperse, J. R., Dubouloz, N., and Sauvaud, J.-A.: Modeling transverse heating and outflow of ionospheric ions from the dayside cusp/cleft: 2 Applications, Ann. Geophys., 21, 1773–1791, 2003b.

Brambilla, M.: Kinetic theory of plasma waves, Oxford Science Pub., 1996.

Chang, T., Crew, G. B., Hershkowitz, N., Jasperse, J. R., Retterer, J. M., and Winningham, J. D.: Transverse acceleration of oxygen ions by electromagnetic ion cyclotron resonance with broadband left-hand-polarized waves, Geophys. Res. Lett., 13, 636–639, 1986.

Cornilleau-Wehrlin, N., Chanteur, G., Perraut, S., Rezeau, L., et al.: First results obtained by the Cluster STAFF experiment, Ann. Geophys., 21, 437–456, 2003.

Crew, G. B., Chang, T., Retterer, J. M., Peterson, W. K., Gurnett, D. A., and Huff, R. L.: Ion cyclotron resonance heated conics: theory and observations, J. Geophys. Res., 95, 3959–3985, 1990.

Dubouloz, N., Delcourt, D., Malingre, M., Berthelier, J.-J., and Chugunin, D.: Remote analysis of cleft ion acceleration using thermal plasma measurements from Interball Auroral Probe, Geophys. Res. Lett., 25, 2925–2928, 1998.

Hamrin, M., Norqvist, P., Hellström, T., André, M., and Ericksson, A. I.: A statistical study of ion energization at 1700 km in the auroral region, Ann. Geophys., 20, 1943–1958, 2002.

Hirahara, M., Mukai, T., Terasawa, T., Machida, S., Saito, Y., Yamamoto, Y., and Kokobun, S.: Cold dense ion flows with multiple components observed in the distance tail lobe by Geotail, J. Geophys. Res., 101, 7769–7784, 1996.

Horwitz, J. L.: Velocity filter mechanism for ion bowl distributions (bimodal conics), J. Geophys. Res., 91, 4513–4523, 1986.

Ichimaru, S.: Basic principles of plasma physics: A statistical approach, edited by Benjamin, W. A., Reading, Mass., 1973.

Kintner, P.: Observations of a velocity shear driven plasma turbulence, J. Geophys. Res., 81, 5114–5122, 1976.

Kintner, P., Bonnell, J., Arnoldy, R., Lynch, K., Pollock, C., and Moore, T.: SCIFER – Transverse ion acceleration and plasma waves, Geophys. Res. Lett., 23, 1873–1876, 1996.

Klumpar, D. M., Peterson, W. K., and Shelley, E. G.: Direct evidence for two-stage (bimodal) acceleration of ionospheric ions, J. Geophys. Res., 89, 10 779–10 787, 1984.

Knudsen, D. J., Whalen, B. A., Abe, T., and Yau, A.: Temporal evolution and spatial dispersion of ion conics: evidence of a polar cusp heating wall, in Solar System Plasmas in Space and Time, Geophys. Monogr. Ser., vol. 84, edited by Burch, J. L. and Waite Jr., J. H., pp 163–169, AGU, Washington D.C., 1994.

Le, G., Blanco-Cano, X., Russell, C. T., Zhou, X.-W., Mozer, F., Trattner, K. J., Fuselier, S. A., and Anderson, B. J.: Electromagnetic ion cyclotron waves in the high-altitude cusp: Polar observations, J. Geophys. Res., 106, 19 067–19 079, 2001.

Lockwood, M., Waite Jr., J. H., Moore, T. E., Johnson, J. F. E., and Chappell, C. R.: A new source of suprathermal O^+ ions near the dayside polar cap boundary, J. Geophys. Res., 90, 4099–4116, 1985a.

Lockwood, M., Chandler, M. O., Horwitz, J. L., Waite Jr., J. H., Moore, T. E., and Chappell, C. R.: The cleft ion fountain, J. Geophys. Res., 90, 9736–9748, 1985b.

Lund, E. J., Moebius, E., Carlson, C. W., Ergun, R. E., Kistler, L. M., Klecker, B., Klumpar, D. M., McFadden, J. P., Popecki, M. A., Strangeway, R. J., and Tung, Y. K.: Transverse ion acceleration mechanism in the aurora at solar minimum: occurrence distributions, J. Atmos. Terr. Phys., 62, 467–475, 2000.

Miyake, W., Mukai, T., and Kaya, N.: On the evolution of ion conics along the field line from EXOS-D observations, J. Geophys. Res., 98, 11 127–11 134, 1993.

Miyake, W., Mukai, T., and Kaya, N.: On the origins of upward shift of elevated (bi-modal) ion conics in velocity space, J. Geophys. Res., 101, 26 961–26 970, 1996.

Miyake, W., Mukai, T., and Kaya, N.: Interplanetary magnetic field control of dayside ion conics, J. Geophys. Res., 105, 23 339–23 344, 2000.

Miyake, W., Matsuoka, A., and Hirano, Y.: A statistical survey of low-frequency electric field fluctuations around the dayside cusp/cleft region, J. Geophys. Res., 108, (A1), doi:10.1029/2002JA009265, 2003.

Moore, T. E., Lundin, R., Alcayde, D., André, M., Ganguli, S. B., Temerin, M., and Yau, A.: Source processes in the high-altitude ionosphere, Space Sci. Rev., 88, 7–84, 1999.

Mukai, T., Kaya, N., Sagawa, E., Hirahara, M., Miyake, W., Obara, T., Miyaoka, T., Machida, S., Yamagishi, H., Ejiri, M., Matsumoto, H., and Itoh, T.: Low energy charged particle observations in the "auroral" magnetosphere: First results from Akebono (Exos-D) satellite, J. Geomag. Geoelectr., 42, 479–496, 1990.

Norqvist, P., André, M., Eliasson, L., Eriksson, A. I., Blomberg, L., Lühr, H., and Clemmons, J. H.: Ion cyclotron heating in the dayside magnetosphere, J. Geophys. Res., 101, 13 179–13 194, 1996.

Øieroset, M., Yamauchi, M., Liszka, L., and Christon, S. P.: Energetic ion outflow from the dayside ionosphere and its relationship to the interplanetary magnetic field and substorm activity, J. Atmos. Terr. Phys., 62, 485–493, 2000.

Opgenoorth, M., Lockwood, M., Alcaydé, D., Donovan, E., et al.: Coordinated ground-based, low-altitude satellite and Cluster observations on global and local scales during a transient post-noon sector excursion of the magnetospheric cusp, Ann. Geophys., 19, 1367–1398, 2001.

Paschmann, G., Treumann, R. A., and Haaland, S.: Auroral plasma physics, Space Sci. Rev., 103, 140–180, 2002.

Peterson, W. K., Collin, H. L., Doherty, M. F., and Bjorklund, C. M.: O+ and He+ restricted and extended (bi-modal) ion conic distributions, Geophys. Res. Lett., 19, 1439–1442, 1992.

Peterson, W. K., Abe, T., André, M., Engebretson, M. J., Fukunishi, H., Hayakawa, H., Matsuoka, A., Mukai, T., Persoon, A. M., Retterer, J. M., Robinson, R. M., Sugiura, M., Tsuruda, K., Wallis, D. D., and Yau, A. W.: Observations of a transverse magnetic field perturbation at two altitudes on the equatoward edge of the magnetospheric cusp, J. Geophys. Res., 98, 21 463–21 470, 1993.

Pinçon, J.-L. and Lefeuvre, F.: Local characterization of homogeneous turbulence in a space plasma from simultaneous measurements of field components at several points in space, J. Geophys. Res., 96, 1789–1802, 1992.

Rème, H., Aoustin, C., Bosqued, J.-M., Dandouras, I., et al.: First multispacecraft ion measurements in and near the Earth's magnetosphere with the identical Cluster ion spectrometry (CIS) experiment, Ann. Geophys., 19, 1303–1354, 2001.

Retterer, J. M., Chang, T., Crew, G. B., Jasperse, J. R., and Winningham, J. D.: Monte Carlo modeling of ionospheric oxygen acceleration by cyclotron resonance with broad-band electromagnetic turbulence, Phys. Rev. Lett., 59, 148–151, 1987.

Sahraoui, F., Pinçon, J.-L., Belmont, G., Rezeau, L., Cornilleau-Wehrlin, N., Robert, P., Mellul, L., Bosqued, J.-L., Balogh, A., Canu, P., and Chanteur, G.: ULF wave identification in the magnetosheath: The k-filtering technique applied to Cluster II data, J. Geophys. Res., 108, (A9), doi:10.1029/2001JA009200, 2003.

Sauvaud, J.-A., Barthe, H., Aoustin, C., Thocaven, J.-J., Rouzaud, J., Penou, E., Popescu, D., Kovrazhkin, R. A., and Afanasiev, K. G.: The ion experiment onboard the Interball-Aurora satellite; initial results on velocity-dispersed structures in the cleft and inside the auroral oval, Ann. Geophys., 16, 1056–1069, 1998.

Seki, K., Hirahara, T., Teresawa, T., Mukai, T., Saito, Y., Machida, S., Yamamoto, T., and Kokobun, T.: Statistical properties and possible supply mechanisms of tailward cold O^+ beams in the lobe/mantle regions, J. Geophys. Res., 103, 4447–4490, 1998.

Seki, K., Elphic, R. C., Thomsen, M. F., Bonnell, J., McFadden, J. M., Lund, E. J., Hirahara, T., Teresawa, T., and Mukai, T.: A new perspective on plasma supply mechanims to the magnetotail from a statistical comparison of dayside mirroring O^+ at low altitudes with lobe/mantle beams, J. Geophys. Res., 107, (A4),

doi:10.1029/2001JA900122, 2002.

Sharp, R. D., Johnson, R. G., and Shelley, E. G.: Observations of an ionospheric acceleration mechanism producing energetic (keV) ions primarly normal to the geomagnetic field direction, J. Geophys. Res., 82, 3324–3328, 1977.

Shelley, E. G., Johnson, R. G., and Sharp, R. D.: Satellite observations of energetic heavy ions during a geomagnetic storm, J. Geophys. Res., 77, 6104–6110, 1972.

Temerin, M.: Evidence for a large bulk ion conic heating region, Geophys. Res. Lett., 13, 1059–1062, 1986.

Thelin, B., Aparicio, B., and Lundin, R.: Observations of upflowing ionospheric ions in the mid-altitude cusp/cleft region with the Viking satellite, J. Geophys. Res., 95, 5931–5939, 1990.

Valek, P. W., Perez, J. D., Jahn, J.-M., Pollock, C. J., Wüest, M. P., Friedel, R. H. W., Moore, T. E., and Peterson, W. K.: Outflow from the ionosphere in the vicinity of the cusp, J. Geophys. Res., 107, (A8), doi:10.1029/2001JA000107, 2002.

Whalen, B. A., Watanabe, S., and Yau, A. W.: Observations in the transverse energization region, Geophys. Res. Lett., 18, 725–728, 1991.

Yau, A. W., Whalen, B. A., McNamara, A. G., Kellog, P. J., and Bernstein, W.: Particle and wave observations of low-altitude ionospheric ion acceleration events, J. Geophys. Res., 88, 341–355, 1983.

Yau, A. W., Peterson, W. K., and Shelley, E. G.: Quantitative parametrization of energetic ionospheric outflow, in modeling magnetospheric plasma, Geophys. Monogr. Ser., vol. 44, edited by Moore, T. E. and Waite Jr., J. H., p. 211, AGU, Washington DC, 1988.